BciD Is a Radical *S*-Adenosyl-ʟ-methionine (SAM) Enzyme That Completes Bacteriochlorophyllide *e* Biosynthesis by Oxidizing a Methyl Group into a Formyl Group at C-7*[S]

Jennifer L. Thweatt[‡], Bryan H. Ferlez[‡], John H. Golbeck[‡§], and 🄳 Donald A. Bryant[‡¶1]

From the Departments of [‡]Biochemistry and Molecular Biology and [§]Chemistry, The Pennsylvania State University, University Park, Pennsylvania 16802 and the [¶]Department of Chemistry and Biochemistry, Montana State University, Bozeman, Montana 59717

Edited by Joseph Jez

Green bacteria are chlorophotorophs that synthesize bacteriochlorophyll (BChl) *c*, *d*, or *e*, which assemble into supramolecular, nanotubular structures in large light-harvesting structures called chlorosomes. The biosynthetic pathways of these chlorophylls are known except for one reaction. Null mutants of *bciD*, which encodes a putative radical *S*-adenosyl-ʟ-methionine (SAM) protein, are unable to synthesize BChl *e* but accumulate BChl *c*; however, it is unknown whether BciD is sufficient to convert BChl *c* (or its precursor, bacteriochlorophyllide (BChlide) *c*) into BChl *e* (or BChlide *e*). To determine the function of BciD, we expressed the *bciD* gene of *Chlorobaculum limnaeum* strain DSMZ 1677[T] in *Escherichia coli* and purified the enzyme under anoxic conditions. Electron paramagnetic resonance spectroscopy of BciD indicated that it contains a single [4Fe-4S] cluster. In assays containing SAM, BChlide *c* or *d*, and sodium dithionite, BciD catalyzed the conversion of SAM into 5′-deoxyadenosine and BChlide *c* or *d* into BChlide *e* or *f*, respectively. Our analyses also identified intermediates that are proposed to be 7^1-OH-BChlide *c* and *d*. Thus, BciD is a radical SAM enzyme that converts the methyl group of BChlide *c* or *d* into the formyl group of BChlide *e* or *f*. This probably occurs by a mechanism involving consecutive hydroxylation reactions of the C-7 methyl group to form a geminal diol intermediate, which spontaneously dehydrates to produce the final products, BChlide *e* or BChlide *f*. The demonstration that BciD is sufficient to catalyze the conversion of BChlide *c* into BChlide *e* completes the biosynthetic pathways for all "*Chlorobium* chlorophylls."

Green bacteria are an eclectic ensemble of anoxygenic chlorophototrophic bacteria that belong to three phyla: Chloroflexi, Chlorobi, and Acidobacteria (1–3). Although physiologically and metabolically diverse, green bacteria share the defining

properties of synthesizing bacteriochlorophyll (BChl)[2] *c*, *d*, or *e* and assembling these BChls into very large light-harvesting complexes known as chlorosomes (4–6). Chlorosomes of green sulfur bacteria (GSB), which can contain up to ~250,000 BChl molecules (4, 7–9), are the largest known light-harvesting antenna complexes, and correspondingly, these structures allow GSB to grow under extraordinarily low light intensities. For example, a population of BChl *e*-producing *Prosthecochloris* sp. BS-1 (formerly *Chlorobium phaeobacteroides* BS-1) stably grows at the chemocline of the Black Sea, which occurs at a depth of ~100–110 m beneath the surface (3, 10, 11). At this depth, the light intensity is nearly 10^6-fold lower than at the surface, ~3 nmol of photons $m^{-2} s^{-1}$ photons/day at the irradiance levels where these bacteria occur (12).

BChls *c*, *d*, and *e* (and BChl *f*, which does not occur naturally) (13–17) comprise the so-called "*Chlorobium* chlorophylls" (Chls). These molecules are not actually BChls but are chlorins that are structurally and spectroscopically more similar to Chl *a* than BChl *a* (18). Mutational analyses made possible by the availability of genome sequences for numerous green bacteria led to the establishment of the pathway for the synthesis of BChls *c* and *d* (12, 18–25). These BChls are synthesized from a pathway that diverges from chlorophyllide (Chlide) *a* (Fig. 1) (18). The first committed step in the biosynthesis of BChl *c*, *d*, and *e* is the removal of the $C-13^2$ carboxymethyl group from Chlide *a* by BciC (23, 26). BchQ and BchR methylate the resulting product at the $C-8^2$ and $C-12^1$ positions, respectively, to produce a family of related homologs (18). These methylation homologs are then hydroxylated at $C-3^1$ by BchF or BchV to produce bacteriochlorophyllide (BChlide) *d* (21, 27–29), and in BChl *c*-producing strains, they are subsequently methylated by BchU at C-20 to produce BChlide *c* homologs (12, 30, 31). Finally, the BChlide *c* or BChlide *d* homologs are esterified with farnesol pyrophosphate by BchK to produce BChl *c* or BChl *d* homologs with differing numbers of methyl groups (20). The methylation reactions catalyzed by BchU, BchQ, and BchR help to tune the absorption properties of BChl *c*, *d*, and *e* in chlorosomes and also lead to inhomogeneous broadening of the near-infrared absorption band of aggregated BChls in chlorosomes

[2] The abbreviations used are: BChl, bacteriochlorophyll; BChlide, bacteriochlorophyllide; BPheide, bacteriopheophorbide; GSB, green sulfur bacteria; Chl, chlorophyll; Chlide, chlorophyllide; SAM, *S*-adenosyl-ʟ-methionine; Et, ethyl; Pr, *n*-propyl; Ib, isobutyl; Np, *neo*-pentyl.

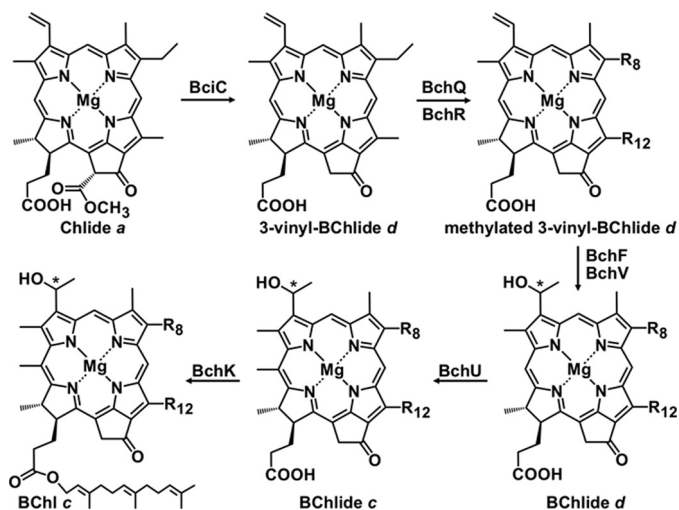# Characterization of Bacteriochlorophyllide e Synthase

FIGURE 1. **Scheme showing the biosynthetic pathway leading from Chlide *a* to BChl *c*.** The side chain at C-8 (R-8) can be ethyl, *n*-propyl, isobutyl, or *neo*-pentyl. The side chain at C-12 (R12) can be methyl or ethyl. The C-8 ethyl group of 3-vinyl-BChlide *d* is methylated by BchQ, and the C-12 methyl group of 3-vinyl-BChlide *d* is methylated by BchR (22). The *asterisk* at C-3[1] indicates a chiral carbon center that can have either *R*- or *S*-stereochemistry. For further details, see the Introduction (3, 18, 24, 25).

(12, 17, 18). Naturally occurring or genetically engineered mutants of *bchU* in formerly BChl *c*-producing strains exclusively synthesize BChl *d* (12, 32–35).

GSB that synthesize either BChl *d* or BChl *c* are green in color, whereas those containing BChl *e* or the unnatural BChl *f* are brown. BChl *e* only differs from BChl *c* by the presence of a formyl group instead of a methyl group at the C-7 position. Similarly, BChl *f* is identical to BChl *d* except for the C-7 formyl group. The available genome sequences of brown-colored GSB contain homologs of all of the genes required for BChl *c* biosynthesis; thus, the BChl *e* biosynthetic pathway is predicted to proceed via the same reactions as that for BChl *c* until the oxidation of the methyl group at the C-7 position (18, 24, 25). A similar oxidation occurs at the C-7 position during the biosynthesis of Chl *b* from Chl *a*; Chl *b* differs from Chl *a* by the presence of a formyl group instead of a methyl group at the C-7 position (36). In the case of Chl *b*, this reaction is catalyzed by an oxygen-dependent enzyme, chlorophyllide *a* oxygenase (37, 38). However, because GSB are strictly anaerobic organisms and their genomes do not encode a homolog of this oxygenase, an as yet uncharacterized enzyme (or enzymes) capable of oxidizing the C-7 methyl group must be responsible for this reaction in the biosynthesis of BChl *e*.

Comparative genomics of brown-colored and green-colored GSB previously identified a conserved gene cluster that could potentially encode an enzyme involved in the conversion of BChlide *c* to BChlide *e* (3, 24, 25, 39). Similar versions of this gene cluster occur in all BChl *e*-producing strains (supplemental Fig. S1), and recent evidence suggests that this conserved gene cluster can be horizontally transferred among GSB by the action of bacteriophages (40). The smallest of these clusters contains about 11 genes extending approximately from a putative radical *S*-adenosyl-L-methionine (SAM) methyltransferase (*bchQ2*) similar to *bchQ* on one border to a gene encoding a homolog of isoprenylcysteine carboxyl methyltransferase, an

enzyme that methylates the C-terminal carboxyl group of pre-nylated proteins (41), near the other border. Previous studies showed that one gene in this cluster, *cruB*, encodes a γ-carotene cyclase that is essential for the synthesis of β-carotene and isorenieratene, carotenoids that are uniquely and nearly universally produced by brown-colored GSB (42). This gene cluster also includes a third homolog of *bchF* and *bchV*, genes that encode C-3 vinyl hydratases (21, 27–29).

The conserved gene cluster in brown-colored GSB notably contains an open reading frame, designated as *bciD*, which encodes a putative radical SAM enzyme. Radical SAM enzymes are capable of performing a variety of radical-mediated reactions under anoxic conditions (43), and they often act as substitutes for oxygen-dependent enzymes in anaerobic organisms. For example, BchE is a radical SAM enzyme that catalyzes the 6-electron oxidation and cyclization of the isocyclic E ring in chlorins in anaerobic chlorophototrophs (3, 18, 24, 25). BchE catalyzes the same reaction as an oxygen-dependent monooxygenase, AcsF, during chlorophyll biosynthesis in aerobic and microaerophilic chlorophototrophs (3, 24, 25, 44, 45).

When the *bciD* gene was inactivated by natural transformation in *Chlorobaculum limnaeum* strain RK-j-1, the resulting strain could no longer synthesize BChl *e* but instead produced BChl *c* (46). Although this result shows that BciD is necessary for the synthesis of BChlide *e*, it does not show that BciD alone is sufficient to catalyze this transformation. Repeated attempts to express the *bciD* gene, as well as some of the surrounding genes from the conserved gene cluster shown in Fig. 2, in *Chlorobaculum tepidum* uniformly failed to produce a strain that could synthesize BChl *e*.[3] Because the phenotype of the *bciD* mutant reported by Harada *et al.* (46) was not verified by complementation, these failures led us to question whether BciD was directly involved in the synthesis of BChl *e*.

In this study, we verified that inactivation of *bciD* in a second strain of *C. limnaeum*, strain DSMZ 1677[T], also led to the synthesis of BChl *c* in the resulting mutant. The *bciD* gene was heterologously expressed in *Escherichia coli*, and the resultant protein was purified and characterized. The purified enzyme contains a single [4Fe-4S] cluster, and when incubated with *S*-adenosyl-L-methionine (SAM) and sodium dithionite, it catalyzed the conversion of BChlide *c* into BChlide *e* and BChlide *d* into BChlide *f*, and it produced 5′-deoxyadenosine as a by-product. These results demonstrate that BciD is a radical SAM enzyme and that it is sufficient to catalyze these two transformations. Thus, the biosynthetic pathway for all *Chlorobium* Chls is now complete.

Results

Inactivation of bciD in C. limnaeum—To confirm the phenotype of the *bciD* mutant described by Harada *et al.* (46), we insertionally inactivated the *bciD* gene in *C. limnaeum* 1677[T]. The mutant was made by conjugation from *E. coli* strain S17-1 carrying the plasmid pCLCON::*bciD* with *C. limnaeum* 1677[T]. This plasmid contained a single homologous region completely internal to the *bciD* gene. After a single homologous recombination event, this should disrupt the *bciD* gene as shown in

---

[3] J. A. Maresca, Z. Liu, J. L. Thweatt, and D. A. Bryant, unpublished results.
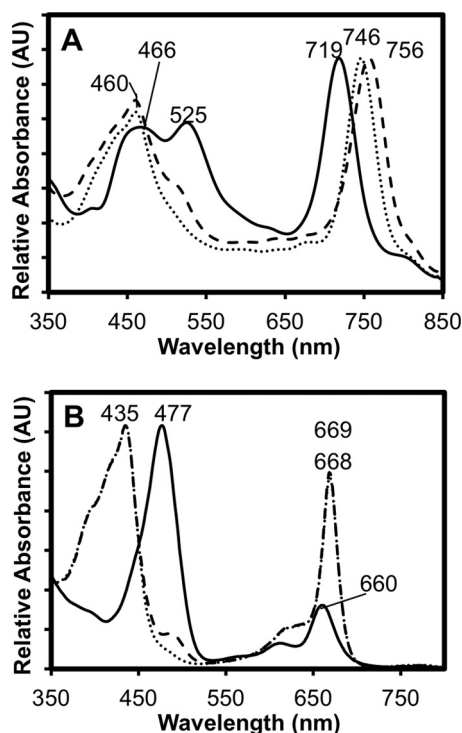
FIGURE 2. **Absorbance spectra of whole cells and pigment extracts.** *A*, whole-cell absorbance spectra of the wild-type (*solid line*) and *bciD* mutant (*dotted line*) strains of *C. limnaeum* compared with wild-type *C. tepidum* (*dashed line*). *B*, absorbance spectra of pigments extracted with 100% methanol from the wild-type (*solid line*) and *bciD* mutant (*dotted line*) strains of *C. limnaeum* compared with wild-type *C. tepidum* (*dashed line*). To facilitate the comparison, the spectra were normalized at the Q_y absorbance maxima for *A* and at the Soret maxima for *B*. *AU*, absorbance units.

TABLE 1

Oligonucleotide primers used in this study

Primer name	Sequence (5' to 3')[a]
CLbciDconSphIF	ATCGATCG**GCATGC**TTAACAAACCACCAGCCTCCG
CLbciDconSalIR	ATCGATCG**GTCGAC**GTTCGAGCCCCATCAGGAT
CLbciDtestF	TAAAGGCGCGACTGCTTTCC
aadAtestR	ATCACTGTGTGGCTTCAGGC
CLbciDNdeIF	GCTATA**CATATG**AGCACAAAAAGGGTT
CLbciDEcoRIR	GCTATA**GAATTC**CTAACAGACGGGGT
CLbciDstopLeuF	GAGCTCGAATTCAAACAGACGGGGTAGGCTTC
CLbciDstopLeuR	GAAGCCTACCCCGTCTGTTTGAATTCGAGCTC

[a] Introduced restriction sites appear in boldface type and are underlined.

supplemental Fig. S2*A*. Transconjugants were screened by PCR with primers bciDtestF and aadAtestR flanking one border of the insertion site (Table 1). Positive transconjugants produced a PCR amplicon of ~1.1 kb as expected (supplemental Fig. S2*B*), whereas wild-type cells did not produce an amplicon. The resulting 1.1-kb PCR product was verified by DNA sequencing.

Cultures of the *bciD* mutant of *C. limnaeum* were green in color, whereas wild-type cultures are brown. To confirm that this color change was due to a change in the BChl content of the *bciD* mutant strain, we compared the UV-visible absorption spectra of whole cells and of the methanol-extracted pigments of wild-type *C. limnaeum*, the *bciD* mutant of *C. limnaeum*, and wild-type *C. tepidum*, a closely related BChl *c*-containing GSB (Fig. 2) (47). Whole-cell spectra (Fig. 2*A*) of the *bciD* mutant very closely matched the spectrum of wild-type *C. tepidum*. The only notable difference was observed around 515 nm, where *C. tepidum* appears to have greater absorbance due to its greater carotenoid content. Similar to *C. tepidum*, the Q_y absorption peak of the green-colored, *bciD* mutant strain shifted to longer wavelength, whereas the Soret absorption peak of the mutant shifted to shorter wavelength. The *bciD* mutant also lacked the secondary absorption peak at around 525 nm that is typical of brown-colored, BChl *e*-containing strains. The UV-visible absorption spectra of the extracted pigments of the *bciD* mutant again matched that of *C. tepidum* except for the carotenoid region (450–500 nm), where *C. tepidum* again exhibited greater absorbance (Fig. 2*B*). These obser-

vations agree with those reported by Harada *et al.* (46) and confirm that inactivation of *bciD* in the *C. limnaeum* strain DSMZ 1677[T] results in loss of the ability to synthesize BChl *e*.

Purification and Characterization of BciD-His[6]—To clarify the role of BciD in the synthesis of BChl *e*, BciD from *C. limnaeum* strain DSMZ 1677[T] was overproduced as a C-terminally His[6]-tagged protein in *E. coli*. The *isc* operon from plasmid pDB1282 was co-expressed with *bciD* to promote [Fe-S] cluster assembly (48). Protein purification was monitored by SDS-PAGE (Fig. 3). After induction, cells contained an abundant protein with an apparent mass of about 44 kDa (Fig. 3, *lane 1*), which is similar to the expected mass of BciD-His[6] (47.3 kDa). Cells were lysed under anoxic conditions, and the lysate was subjected to ultracentrifugation to separate the soluble fraction from unbroken cells, membranes, and other debris. Although some of the protein formed inclusion bodies (data not shown), a sufficient amount of the protein of interest was observed in the soluble fraction (Fig. 3, *lane 2*) to justify continuing with the purification. The protein was purified by nickel affinity chromatography under strictly anoxic conditions. After concentration and buffer exchange, a relatively pure protein of roughly the expected size was obtained (Fig. 3, *lane 7*). This protein was subjected to in-gel trypsin digestion, and the resulting peptides were analyzed by mass spectrometry, and the analysis confirmed that the protein was BciD-His[6].

As expected for a radical SAM protein, which by precedent is predicted to contain at least one [4Fe-4S] cluster, the purified BciD-His[6] protein was brown in color. Fig. 4 shows the UV-visible absorption spectrum of the as-isolated protein, which had broad, weak absorbance characteristics of an $S \rightarrow Fe$ charge transfer band with a maximum at about 400 nm. After reconstitution with iron and sulfide as described under "Experimental Procedures," this absorbance band increased substantially (roughly 2-fold), indicating that the Fe/S cluster binding site in the as-isolated protein was not completely occupied. To confirm the presence of the predicted [4Fe-4S] cluster, we measured the EPR spectra of as-isolated and reconstituted BciD. Fig. 5 shows the difference spectra of protein samples reduced with 5 mM dithionite minus the spectra of the untreated samples. In the untreated (oxidized) samples, no EPR resonances were observed; however, after reduction, as seen in the difference spectra, both the as-isolated and the reconstituted protein showed spectral features with axial symmetry and g values of 2.038 and 1.945. These spectra correspond to those typical of proteins with a single, reduced [4Fe-4S] cluster as predicted for this putative radical SAM enzyme.

BciD-His[6] Activity Assay with BChlide c—Activity assays for BciD-His[6] were performed under strictly anoxic conditions at
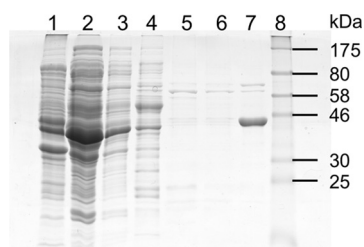
FIGURE 3. **SDS-PAGE analysis of fractions from the purification of recombinant BciD-His₆.** *Lane 1*, whole-cell extract of the BciD-His₆ expression strain; *lane 2*, crude supernatant after low speed centrifugation to remove membranes and debris; *lane 3*, flow-through fraction from nickel chelation chromatography; *lane 4*, column wash, fraction 1; *lane 5*, column wash, fraction 2; *lane 6*, column wash, fraction 3; *lane 7*, purified BciD-His₆; *lane 8*, protein mass markers. BciD-His₆ has an apparent mass of about 44 kDa.
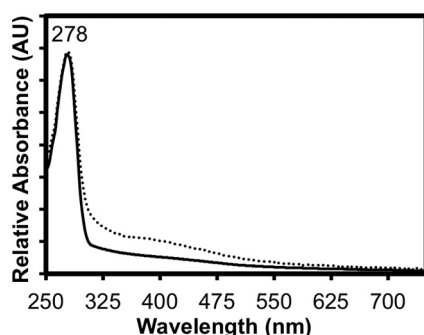

FIGURE 4. **UV-visible absorbance spectra of as-isolated and reconstituted recombinant BciD-His₆.** The spectra for as-isolated (*solid line*) and reconstituted BciD-His₆ are shown. To facilitate comparison, the spectra were normalized at the UV absorbance maxima. *AU*, absorbance units.
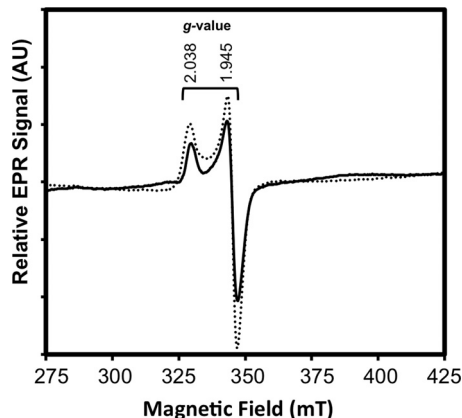

FIGURE 5. **EPR spectra of as-isolated and reconstituted recombinant BciD-His₆.** EPR spectra of as-isolated (*solid line*) and reconstituted recombinant BciD-His₆ (*dotted line*). Each spectrum represents the difference spectrum between the reduced sample and the untreated (oxidized) sample. The samples were reduced by the addition of 5 mM sodium dithionite. The concentration of reconstituted BciD was 25 μM, and the concentration of as-isolated BciD was 55 μM. Spectrometer conditions are provided under "Experimental Procedures." The g values of the axial signal are indicated *above* the spectra. *AU*, absorbance units; mT, millitesla.

room temperature. Purified BciD-His₆ was incubated with a mixture of methylation homologs of BChlide c or BChlide d, SAM as a cofactor, and sodium dithionite as reductant. Control reactions without added BciD-His₆ were always prepared in parallel. The pigments present in the mock control reaction were compared with those present after incubation with the enzyme by reversed-phase HPLC, and the masses of the products and reactants were determined by mass spectrometry in

parallel reactions. Fig. 6*A* shows the HPLC elution profile of the pigments present in the samples containing BChlide c as the substrate. The *dotted line* contains a series of peaks that make up the substrate; the peaks at 22.3, 26.1, 29.0, 32.3, and 35.0 min account for the various methylation homologs of BChlide c, whereas the peaks at 36.9, 39.6, 40.3, and 43.0 min represent the methylation homologs of BPheide c, a breakdown product of BChlide c from which the central magnesium atom has been lost. As shown in Fig. 6*B*, the UV-visible spectra of BChl c in methanol and the in-line absorption spectrum of the major BChlide c substrate peak eluting at 26 min are essentially identical. The *solid line* in the HPLC elution profiles in Fig. 6*A* shows a series of peaks that are derived from reaction products and unreacted substrate molecules. The peaks at 12.1, 15.3, 16.6, 18.7, 20.0, and 21.6 min uniquely occur in the elution profile of the products (Fig. 6*A* and Table 2). The earlier elution times of the product peaks are consistent with the increased hydrophilicity expected for BChlide e due to replacement of the methyl group by the formyl group at the C-7 position. In Fig. 6*C*, the UV-visible spectra of the major 20-min product peak and the 26-min substrate peak are compared. Compared with the substrate BChlide c, the Q_y absorption peak of the product is blue-shifted, and its Soret peak is red-shifted, as expected for BChlide e. In Fig. 6*D*, the spectra of the 20-min product and BChl e in methanol are compared, which confirms that the reaction product is BChlide e. Mass spectrometry showed that the masses of the BChlide c substrate peaks increase in 14-Da increments as they become more hydrophobic because of the additional methyl groups of the homologs (Table 2). Correspondingly, the product peaks are shifted toward earlier elution times due to greater hydrophilicity, and these compounds had masses that were 14 Da larger than the corresponding substrate peak, which diminished in intensity during the reaction (Table 2). This is consistent with the results expected if the methyl group of BChlide c was transformed into a formyl group to yield BChlide e.

In a separate analysis by HPLC, SAM was consumed, and 5'-deoxyadenosine was formed in the complete reaction containing BciD-His₆, but these changes were not observed in a control reaction lacking the enzyme (Fig. 7). All of these observations are consistent with the expected functioning of a radical SAM enzyme that converts BChlide c into BChlide e.

The minor product peak at 15.2 min is particularly noteworthy. This product is obviously more hydrophilic than the major BChlide e product peak at 20 min. The in-line absorption spectrum of this product, with maxima at 441 and 666 nm (Fig. 6*E* and Table 2), more closely resembled the spectrum of the BChlide c substrate than the BChlide e product but was nevertheless distinct. The mass of this compound was 2 Da larger than that of the BChlide e product at 20 min. These properties are consistent with those expected for 7¹-hydroxy-BChlide c. These observations strongly imply that BciD is a radical SAM enzyme that acts by catalyzing two consecutive hydroxylation reactions of the C-7 methyl group.

BciD-His Activity Assay with BChlide d—A similar activity analysis is shown in Fig. 8 for the complete reaction and control with BChlide d as the substrate. Similar to the results shown for BChlide c in Fig. 6, the substrate contained methylation homo-
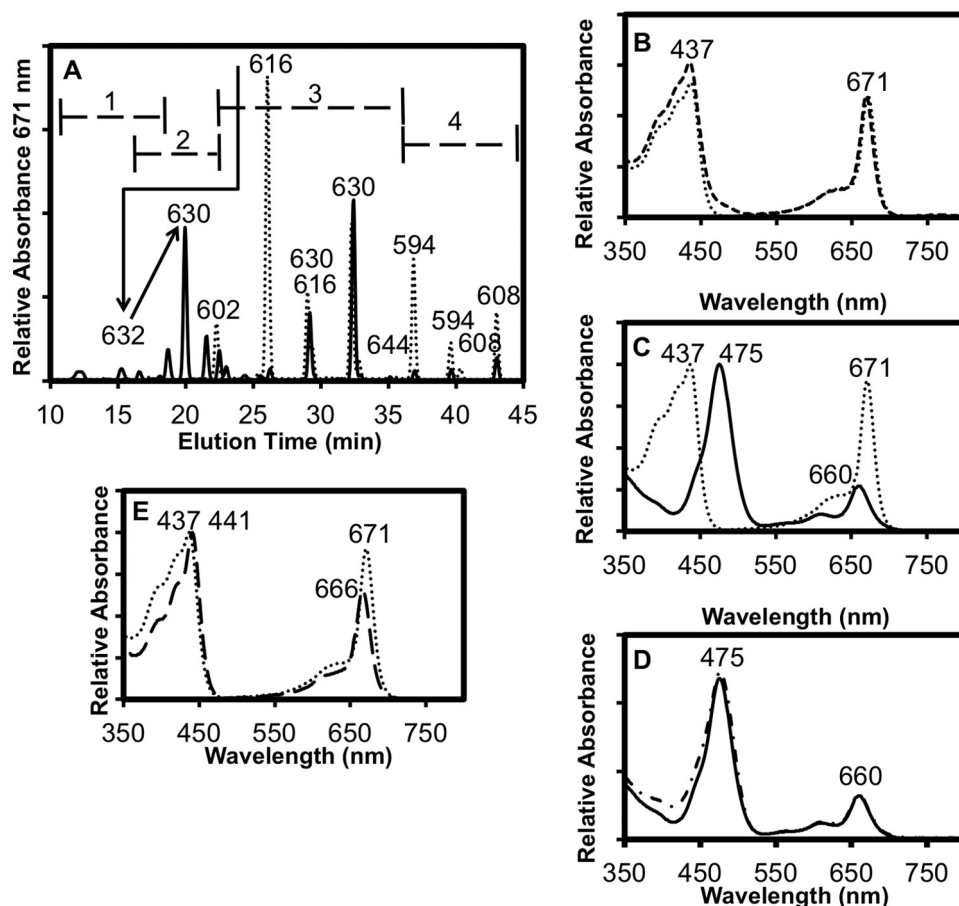
FIGURE 6. **Reversed-phase HPLC analysis of BciD reaction with BChlide c.** *A*, reversed-phase HPLC elution profile of BciD control reaction (*dotted line*) and the 1-h reaction (*solid line*) using BChlide *c* as the substrate. Masses of selected peaks are indicated in Da *above* the peaks. The *numbered ranges* indicated by *brackets* in *A* indicate the ranges at which 7–1-OH-BChlide *c* (*range 1*), BChlide *e* (*range 2*), BChlide *c* (*range 3*), and BPheide *c* (*range 4*) methylation homologs elute (also see Table 2). The *arrows* indicate the conversion of [Pr,Et]-BChlide *c* into 7^1-OH-BChlide *c* and then to BChlide *e*. *B*, comparison of the absorbance spectra of the 26.1-min substrate peak in *A* (*dotted line*) with BChl *c* in methanol (*dashed line*). *C*, comparison of the absorbance spectra of the 26.1-min substrate peak in *A* (*dotted line*) and the 20.0-min BChlide *e* product peak (*solid line*). *D*, comparison of the absorbance spectra of the 20.0-min product peak (*solid line*) and BChl *e* in methanol (*dashed-dotted line*). *E*, comparison of the 26.1-min substrate peak (*dotted line*) with the 15.3-min product peak (*long-dashed line*). For identities of compounds and additional information, see Table 2.

TABLE 2

Summary of properties and assignments of peaks in BciD reaction with BChlide c (see Fig. 6)

ND, not determined; Me, methyl; Et, ethyl; Pr, *n*-propyl; Ib, isobutyl; Np, *neo*-pentyl.

	Control reaction, BChlide *c*				Complete reaction, BChlide *c*			
Peak number	Retention time	Absorbance peaks	Mass	Proposed pigment assignment	Retention time	Absorbance peaks	Mass	Proposed pigment assignment
	min	*nm*	*Da*		*min*	*nm*	*Da*	
1					12.1	440, 666	ND	7^1-OH-BChlide *c*
2					15.3	441, 666	632	7^1-OH-[Pr,Et]-BChlide *c*
3					16.6	475, 660	ND	BChlide *e*
4					18.7	441, 666	646	7^1-OH-[Ib,Et]-BChlide *c*
5					20.0	475, 660	630	[Pr,Et]-BChlide *e*
6					21.6	442, 474, 666	ND	Mixed peak
7	22.3	437, 671	602	[Et, Et]-BChlide *c*	22.5	437, 671	602	[Et,Et]-BChlide *c*
8	26.1	437, 671	616	[Pr, Et]-BChlide *c*	26.3	437, 671	616	[Pr,Et]-BChlide *c*
9	29	437, 671	616, 630	BChlide *c*	29.2	437, 671	616, 630	BChlide *c*
10	32.3	437, 671	630	[Ib, Et]-BChlide *c*	32.5	437, 671	630	[Ib,Et]-BChlide *c*
11	32.8	413, 670	580	[Et, Et]-BPheide *c*	32.9	413, 670	580	[Et,Et]-BPheide *c*
12	35	438, 671	644	[Np, Et]-BChlide *c*	35.1	438, 671	644	[Np,Et]-BChlide *c*
13	36.9	414, 670	594	[Pr, Et]-BPheide *c*	37.0	414, 670	594	[Pr,Et]-BPheide *c*
14	39.6	414, 670	594	BPheide *c*	39.7	414, 670	594	BPheide *c*
15	40.3	414, 670	608	BPheide *c*	40.4	413, 670	608	BPheide *c*
16	43	414, 670	608	[Ib, Et]-BPheide *c*	43.1	414, 670	608	[Ib,Et]-BPheide *c*

logs of BChlide *d* and small amounts of BPheide *d* (Fig. 8*A*), and as expected, the UV-visible spectrum of the major substrate peak at 21.6 min matched that of BChl *d* in methanol (Fig. 8*B*). The major product peak at 18.9 min differs from BChlide *d* (Fig.

8*C*) but matches the spectrum of BChl *f*, as expected for the conversion of BChlide *d* to BChlide *f* (Fig. 8*D*). The main product peak appears at 18.9 min and appears to come from the second most abundant substrate peak at 25.4 min. The shift to
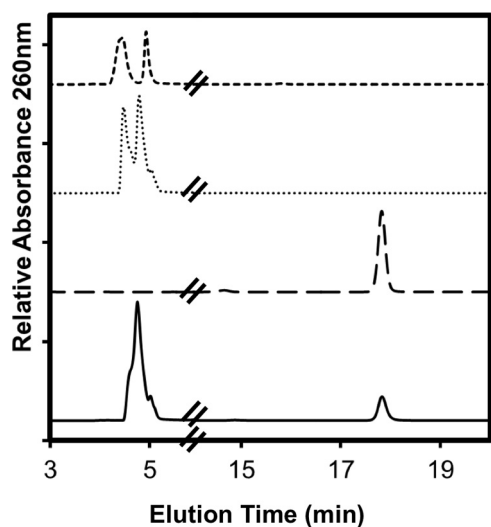
FIGURE 7. **Reversed-phase HPLC analysis of 5′-deoxyadenosine produced by BciD during reaction with BChlide c.** Shown is a reversed-phase HPLC elution profile of SAM standard (*dashed line*), 5′-deoxyadenosine standard (*long-dashed line*), 1-h control reaction with BChlide c (*dotted line*), and 1-h complete reaction with BciD (*solid line*) using BChlide c as the substrate. SAM (4.5 min) is consumed, and 5′-deoxyadenosine (17.8 min) is produced during the reaction.

an earlier elution time, from 25.4 min for the substrate peak to 18.9 min for the product, as well as the increase in mass by 14 Da, are the expected results if the C-7 methyl group of BChlide *d* has been transformed into a formyl group to produce BChlide *f* (Table 3). These data establish that BciD is not only necessary for the conversion of BChlide *c* and *d* into BChlide *e* and *f*, respectively, but it is sufficient to catalyze these transformations. As observed with BChlide *c* as substrate, a product peak at 14 min was probably due to 7^1-hydroxy-BChlide *d*. This product was more hydrophilic than the BChlide *f* products and had an absorption spectrum with maxima at 433 and 653 nm (Table 3 and Fig. 8*E*) that was more similar to BChlide *d* than to BChlide *f*. These data strongly imply that BciD-His$_6$ sequentially hydroxylates the C-7 methyl group twice during the synthesis of BChlide *f*.

Discussion

The goal of this study was to clarify the role of BciD in the biosynthetic pathway of BChl *e*. Previous studies (46) had shown that inactivation of the *bciD* gene in *C. limnaeum* prevented the biosynthesis of BChl *e*, resulting in production of BChl *c* in the mutant. However, repeated attempts to express *bciD* in *C. tepidum* failed to produce strains capable of BChl *e* synthesis or related compounds (*e.g.* 7^1-hydroxy-BChl *c*). Therefore, we first verified the phenotype reported for a *bciD* mutant of *C. limnaeum* strain RK-j-1 (46). The results presented in Fig. 2 agree well with those from the previous study and show that inactivation of *bciD* of *C. limnaeum* DSMZ 1677^T also produced a BChl *c*-producing mutant strain.

The EPR spectra of recombinant BciD-His$_6$ had features that are consistent with the presence of a single [4Fe-4S] cluster in the enzyme. In radical SAM enzymes, the SAM-activating [4Fe-4S] cluster has a binding motif consisting of three cysteines, and the canonical motif is CXXXCXXC. Supplemental Fig. S3 shows a multiple sequence alignment of BciD from four

brown-colored, BChl *e*-producing GSB. These proteins contain five conserved cysteine residues at positions 78, 124, 133, 136, and 261; we propose that the cysteines at positions 124, 133, and 136 are ligands to the observed [4Fe-4S] cluster. The proposed roles of these three cysteine residues in ligating the [4Fe-4S] cluster in BciD will be tested by site-specific mutagenesis in future studies. In the presence of SAM and dithionite, BciD-His$_6$ converted BChlide *c* and BChlide *d* to BChlide *e* and BChlide *f*, respectively. We additionally observed the formation of more hydrophilic products. Based upon the elution properties, absorption spectra, and masses of these compounds, we propose that they are methylation homologs of 7^1-OH BChlide *c* and 7^1-OH BChlide *d*, respectively (Tables 2 and 3). Finally, we observed that BciD consumed SAM as a cofactor and produced 5′-deoxyadenosine as a by-product of the reaction. Taken together, these observations lead us to conclude that BciD is a radical SAM enzyme with a non-canonical cysteine motif of three cysteine residues that ligates a SAM-activating [4Fe-4S] cluster and that catalyzes the conversion of the C-7 methyl group of BChlide *c* or *d* to the formyl group of BChlide *e* or BChlide *f* via consecutive hydroxylation reactions (Fig. 9).

Given that BciD appears to be sufficient to convert BChlide *c* into BChlide *e in vitro*, it is still a mystery why expression of *bciD* in the BChl *c*-containing GSB *C. tepidum* has repeatedly failed to produce BChls containing either hydroxymethyl or formyl side chains at C-7. One possible explanation is that *C. limnaeum* and *C. tepidum* have significantly different optimal growth temperatures, and BciD might not be active at higher temperature. *C. tepidum* is routinely grown at 40–48 °C in the laboratory, whereas *C. limnaeum* is typically grown at 25–30 °C. However, we were still able to observe BciD-His$_6$ activity *in vitro* at 40 °C (data not shown), which seemingly excludes this explanation. Alternatively, although it seems unlikely, one could postulate that there is no appropriate electron donor for this reaction in *C. tepidum*. Obviously, sodium dithionite is not the biological electron donor for this reaction *in vivo* in *C. limnaeum*. GSB, including *C. tepidum*, contain small, highly abundant soluble ferredoxins that typically serve this function (3, 49, 50). A counterargument to this point is that there is no gene encoding a ferredoxin or other potential electron donor protein encoded in the gene cluster that is specifically found in brown-colored, BChl *e*-producing GSB strains. Although it again seems unlikely because *C. tepidum* produces many Fe/S proteins, it is possible that the [4Fe-4S] cluster of BciD is unable to assemble, or that BciD is unable to fold properly, in the context of the *C. tepidum* cytoplasm.

An alternative explanation is that there is a biosynthetic problem downstream from BciD and BChlide *e* that prevents the accumulation of BChl *e* in *C. tepidum*. Specifically, the enzymes responsible for adding the esterifying alcohols to Chls and BChls show considerable specificity for the (B)Chlide substrate but usually have broader specificity for the esterifying alcohol (20, 51–53). In *C. tepidum* BchK is responsible for the addition of the farnesyl tail to BChl *c*, and ChlG and BchG add phytadienol and phytol to Chl *a* and BChl *a*, respectively (20). A comparative analysis of the genomes of GSB shows that all have at least three esterifying enzymes: BchK, ChlG, and BchG.
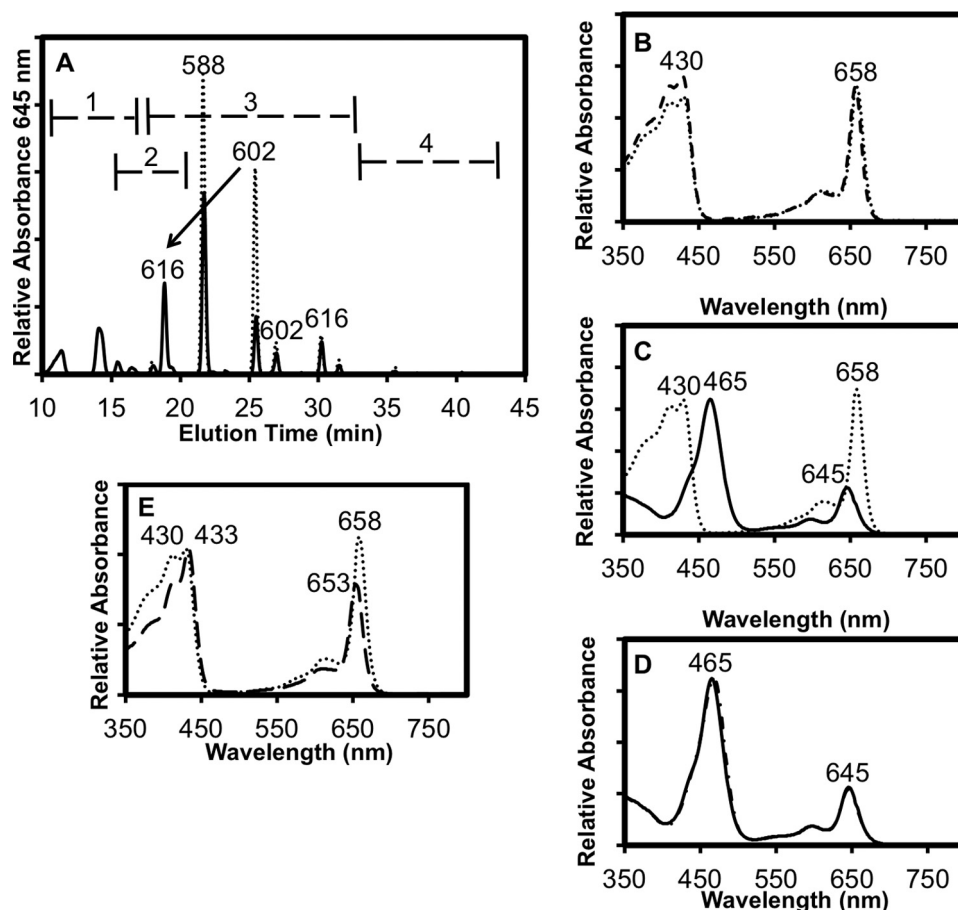
FIGURE 8. **Reversed-phase HPLC analysis of BciD reactions with BChlide d.** *A*, reversed-phase HPLC elution profile of control reaction (*dotted line*) and the 1-h complete reaction (*solid line*) using BChlide *d* as the substrate for BciD. The *numbered ranges* indicated by *brackets* in *A* indicate the ranges at which 7–1-OH-BChlide *d* (*range 1*), BChlide *f* (*range 2*), BChlide *d* (*range 3*), and BPheide *d* (*range 4*) methylation homologs elute (also see Table 2). The *arrow* indicates the conversion of [Pr,Et]-BChlide *d* into [Pr,Et]-BChlide *f*. Masses of selected peaks in Da are indicated *above* the peaks. *B*, comparison of the absorbance spectra of the 21.6-min substrate peak in *A* (*dotted line*) with BChl *d* in methanol (*dashed line*). *C*, comparison of the absorbance spectra of the 21.6-min substrate peak in *A* (*dashed line*) and the 18.9-min product peak (*solid line*). *D*, comparison of the absorbance spectra of the 18.9-min product peak (*solid line*) and BChl *f* in methanol (*dashed-dotted line*). *E*, comparison of the absorption spectrum of the product peak at 16.5 min (7^1-OH-BChlide *d*) with the absorption spectrum of the substrate peak at 21.6 min ([Et,Et]-BChlide *d*). See Table 3 for identities of compounds and additional information.

TABLE 3

Summary of properties and assignments of peaks in BciD reaction with BChlide *d* (see Fig. 8)

Masses in parentheses are inferred from those identified for the control reaction. ND, not determined; Me, methyl; Et, ethyl; Pr, *n*-propyl; Ib, isobutyl.

Peak number	Control reaction, BChlide *d*				Complete reaction, BChlide *d*			
	Retention time	Absorbance peaks	Mass	Proposed pigment assignment	Retention time	Absorbance peaks	Mass	Proposed pigment assignment
	min	*nm*	*Da*		*min*	*nm*	*Da*	
1					11.4	433, 653	ND	7^1-OH-BChlide *d*
2					14.1	433, 653	ND	7^1-OH-BChlide *d*
3					15.5	465, 646	ND	[Et,Et]-BChlide *f*
4					16.5	433, 653	ND	7^1-OH-BChlide *d*
5	18.0	430, 659	574	[Me,Et]-BChlide *d*	18	430, 659	(574)	[Me,Et]-BChlide *d*
6					18.9	465, 645	616	[Pr,Et]-BChlide *f*
7	21.6	429, 658	588	[Et,Et]-BChlide *d*	21.7	430, 658	588	[Et,Et]-BChlide *d*
8	25.4	430, 658	602	[Pr,Et]-BChlide *d*	25.5	430, 659	(602)	[Pr,Et]-BChlide *d*
9	26.9	430, 658	602	BChlide *d*	27	430, 658	(602)	BChlide *d*
10	30.2	430, 659	616	[Ib,Et]-BChlide *d*	30.2	430, 659	616	[Ib,Et]-BChlide *d*
11	31.5	408, 659	566	[Et,Et]-BPheide *d*	31.5	408, 659	566	[Et,Et]-BPheide *d*
12	35.6	408, 660	580	[Pr,Et]-BPheide *d*	35.6	408, 660	(580)	[Pr,Et]-BPheide *d*

Interestingly, *C. limnaeum* has two paralogs of the *bchK* gene; one paralog encodes BchK1, which is very similar to the enzyme found in *C. tepidum*, but paralog BchK2 is much more divergent (supplemental Fig. S4). Moreover, all brown-colored, BChl *e*-producing GSB species contain a BchK enzyme that is phylogenetically distant from the BchK of *C. tepidum*. These obser-

vations suggest that a possible problem in producing BChl *e* in *C. tepidum* might result from an incompatibility between the esterifying enzyme (BchK) in *C. tepidum* and the BChlide *e* substrate. If this is correct, then it might be possible to circumvent this problem by expressing the *bchK2* gene of *C. limnaeum* together with *bciD* in *C. tepidum*. The construction of a brown-
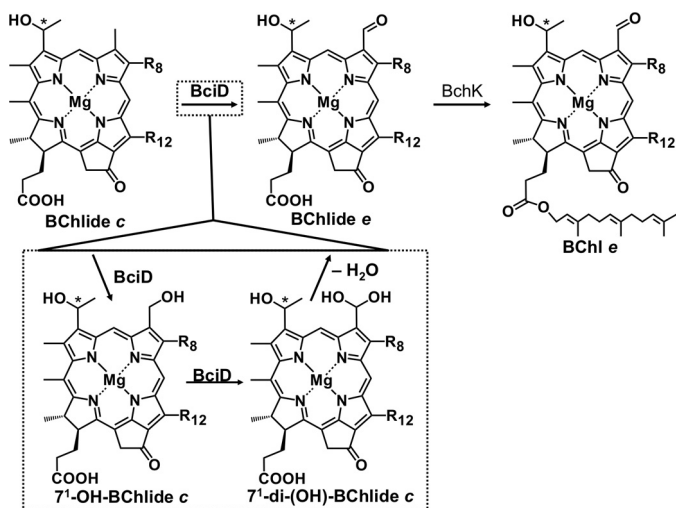
FIGURE 9. **Proposed reaction scheme for BciD and BchK to convert BChlide *c* into BChl *e*.** BciD is proposed to act by sequential hydroxylation of the C-7 methyl group, producing 7^1-monohydroxy and 7^1-dihydroxy derivatives of BChlide *c* as intermediates. Spontaneous dehydration of the geminal-diol intermediate produces the 7-formyl group of BChlide *e*. BChlide *e* is esterified *in vivo* by BchK to produce BChl *e*.

colored, BChl *e*-producing strain of *C. tepidum* would be very useful for physiological and biophysical studies on the specific role(s) of the BChl *e* in adaptation of GSB to growth at very low light intensities.

When assembled into chlorosomes, BChls *c*, *d*, and *e* have distinctive absorption features that are associated with specific light niches in nature (4, 6). In aquatic systems, organisms with chlorosomes containing BChl *d* typically occur at shallower depths than organisms containing BChl *c* (12, 54–56). A similar pattern is observed in benthic mat systems in chlorophototrophic mats associated with alkaline siliceous hot springs in Yellowstone National Park (57, 58). When BChl *e* assembles into supramolecular aggregates in chlorosomes, an emergent absorption band appears at about 525 nm (see Fig. 4) that allows these organisms to very efficiently harvest blue light (6). Such organisms are also typically able to grow at greater depths and at remarkably low light intensities (10–13, 54–56). Thus, the ability to synthesize BChl *e* is associated with the ability to inhabit a light niche that is inaccessible to other chlorophototrophs. Should the *bciD* gene be horizontally transferred to a recipient capable of BChl *c* synthesis, the ability to synthesize BChl *e* would allow that organism to modify its light-harvesting chlorosomes and invade niches with lower light intensities and fewer competitors.

Evidence exists for horizontal gene transfer for the entire gene cluster that includes *bciD* and *cruB* (40). In Lake Cisó in Spain, the resident population of GSB recently shifted from green to brown, and a metagenomic analysis showed that the genome of the brown-colored organism was extremely similar to the type strain of *Chlorobium luteolum* DSM 273[T], a green-colored, BChl *c*-producing strain (3). Some evidence pointed to a DNA phage as a possible vector for this transfer (40). Interestingly, *Chlorobium luteolum* DSM 273[T] has two *bchK* genes, one of which is similar to the *bchK* gene of *C. tepidum* and one of which (*bchK2*) belongs to the clade of enzymes that are found in brown-colored, BChl *e*-producing GSB strains (supplemen-

tal Fig. S4). The presence of a *bchK2* gene, the product of which can presumably esterify BChlide *e* with farnesol, might "predispose" *Chlorobium luteolum* to transformation from a BChl *c*-producing into a BChl *e*-producing strain by the acquisition of *bciD*, although the horizontally transferred, conserved gene cluster does not include a gene for a chlorophyll synthase. These ideas can be tested in future studies by inactivating the *bchK1* and *bchK2* genes in *C. limnaeum* as well as by introducing the *bciD* gene into *C. tepidum* in combination with each of the two *bchK* genes encoding the two paralogous esterification enzymes of *C. limnaeum*.

Questions remain about the detailed mechanism of hydroxylation, the source of oxygen for this reaction (presumably water), and the structure of the BciD enzyme. BciD is the first radical SAM enzyme of its subclass to be characterized. A blastp comparison of BciD against the UCSF structure-function linkage database showed that BciD is most closely related to uncharacterized subgroup 20 and uncharacterized subgroup 11 of the radical SAM superfamily (59). A blastp search of the NCBI protein database with the BciD query returned 928 sequences with an *e* value <0.001; however, none of these proteins have been characterized *in vitro*. The blastp search also showed that BciD has similarity to the following conserved domains: Elp3, rSAM_MSMEG_0568, Radical_SAM, and BioB. These conserved domains correspond to the superfamily denoted Elongator protein 3/MiaB/radical SAM, which contains several radical SAM enzyme families, the protein family radical SAM MSMEG_0568, which has no characterized function, the radical SAM superfamily, and a domain found in biotin synthase and related enzymes. The absence of obviously close relatives makes the BciD enzyme interesting for future study, not just from the perspective of BChl synthesis, but also from the perspective of radical SAM biochemistry more broadly.

Experimental Procedures

Strains Used in This Study—C. limnaeum strain DSMZ 1677[T] (47) was obtained from the culture collection of Dr. Johannes Imhoff (University of Kiel, Germany). *C. limnaeum* is capable of thiosulfate utilization (13), and it was routinely grown on medium CL used for *C. tepidum* (60, 61) at irradiances of 10–100 μmol of photons m^{-2} s^{-1} provided by either tungsten or cool white fluorescent lamps. *C. limnaeum* cells were grown at room temperature in CL medium in liquid and the same medium solidified with 1.5% (w/v) Bacto™ Agar (BD Biosciences) in a Coy anoxic chamber under an atmosphere of $N_2/CO_2/H_2$ (80:10:10, v/v/v). Plates were further enclosed in Gas-Pak jars containing thioacetamide as described previously (61). The complete genome of this organism has been sequenced and is available in GenBank™ as accession number CP017305.[4]

Routine cloning to produce constructions for gene inactivation were performed using chemically competent α-select *Escherichia coli* cells (Bioline, Taunton, MA). The *E. coli* strain used for conjugation was S17-1 (62), and *E. coli* strain BL21 (DE3) was used for expression of the *bciD* gene. *E. coli* strains

---

[4] M. Tank, Z. Liu, L. P. Thomsho, S. C. Schuster, and D. A. Bryant, manuscript in preparation.

were grown in Luria-Bertani (LB) medium containing antibiotics as required. For overproduction of BciD, the medium was supplemented with ferric ammonium citrate (100 μM) and L-cysteine (100 μM). Antibiotic concentrations for *E. coli* were as follows: spectinomycin, 100 μg ml^{-1}; ampicillin, 100 μg ml^{-1} streptomycin, 50 μg ml^{-1}; and kanamycin, 50 μg ml^{-1}. Antibiotic concentrations for *C. limnaeum* grown on solid medium were as follows: spectinomycin, 200 μg ml^{-1}; streptomycin, 100 μg ml^{-1}; kanamycin, 30 μg ml^{-1}. When grown in liquid medium, antibiotic concentrations for *C. limnaeum* were as follows: spectinomycin, 37.5 μg ml^{-1}; streptomycin, 18.75 μg ml^{-1}.

Cloning and Inactivation of bciD in C. limnaeum—Inactivation of the *bciD* gene of *C. limnaeum* strain DSMZ 1677^{T} was performed by conjugative gene transfer essentially as described (13). A gene-internal region of the *bciD* gene was amplified by PCR using oligonucleotide primers CLbciDconSphIF and CLbciDconSalIR (Table 1) and cloned into the SphI and SalI sites of the conjugation vector pCLCON (13) to create vector pCLCON::*bciD* (supplemental Fig. S2*A*) The resulting plasmid was transformed into *E. coli* strain S17-1. Conjugation between the S17-1 strain and wild-type *C. limnaeum* was performed as described previously (13), and transconjugants were selected on solid medium containing spectinomycin, streptomycin, and kanamycin. Transconjugant colonies were screened by PCR using oligonucleotide primers CLbciDtestF and aadAtestR (Table 1) that flank one border of the gene insertion site; amplicons were analyzed by agarose gel electrophoresis (supplemental Fig. S2 *B*), and positive PCR amplicons were confirmed by DNA sequencing at the Genomics Core Facility (Pennsylvania State University, University Park, PA).

Cloning and Heterologous Expression of bciD in E. coli—The *bciD* gene from *C. limnaeum* was amplified via PCR using oligonucleotide primers CLbciDNdeIF and CLbciDEcoRIR (Table 1). The resulting PCR amplicon and plasmid pET26b were digested with NdeI and EcoRI, and the products were ligated to insert the *bciD* gene upstream of the sequence for a C-terminal His$_6$ tag. Site-directed mutagenesis was used to change the *bciD* stop codon to a leucine codon using the QuikChange II mutagenesis kit (Agilent Technologies, Santa Clara, CA) and oligonucleotide primers CLbciDstopLeuF and CLbciDstopLeuR (Table 1). The complete coding sequence and the downstream flanking region encoding the His$_6$ tag in the resulting plasmid, pET26b(*bciD*-His$_6$), were confirmed by DNA sequencing at the Genomics Core Facility.

The expression and purification of BciD-His$_6$ was modified from protocols used for other radical SAM enzymes (48). The expression plasmid pET26b(*bciD*-His$_6$) was transformed into *E. coli* strain BL21 (DE3) together with plasmid pDB1282, which contains part of the *Azotobacter vinelandii isc* operon for [Fe-S] cluster assembly under the control of an arabinose repressor and operator (48, 63, 64). A starter culture of the expression strain was grown overnight at 37 °C in LB medium supplemented with ampicillin and kanamycin. A 2.5-liter culture in minimal medium containing 2% (v/v) glycerol, ampicillin, and kanamycin was inoculated with a 25-ml overnight culture. The culture was grown at 37 °C with gentle rotation to an OD$_{600}$ of 0.2–0.3, and expression of the *isc* operon of pDB1282

was induced with 0.2% L-arabinose after supplementing the medium with ferric ammonium citrate (100 μM) and cysteine (100 μM). After the addition of arabinose, cells were grown at 37 °C to an OD$_{600}$ of 0.7–0.8 and then cooled to ~18 °C. Finally, BciD-His$_6$ production was induced by adding isopropyl-β-D-1-thiogalactopyranoside (50 μM). After further incubation at 18 °C for 16–20 h, cells were harvested by centrifugation and either immediately transferred to an anoxic chamber or frozen and placed at −80 °C for short term storage before lysis.

BciD Purification—Buffers used for purification of BciD were made in an anoxic chamber by dissolving the solid materials in anoxic water. The cell pellet was thawed on ice in the anoxic chamber, and cells were resuspended in lysis buffer containing 50 mM HEPES, pH 7.5, 300 mM NaCl, 20 mM imidazole, and 10 mM 2-mercaptoethanol. Lysozyme was added to 1 mg ml^{-1}, and the suspension was incubated with rocking for 30 min at room temperature. Cells were cooled on ice and then lysed by sonication. Lysed cells were transferred to ultracentrifuge tubes and sealed inside the anoxic chamber before pelleting the cell debris by ultracentrifugation. The tubes were returned to the anoxic chamber, and the soluble fraction was loaded onto a nickel affinity column pre-equilibrated with lysis buffer. The column was washed three times with three volumes of wash buffer. Wash buffer contained 50 mM HEPES, pH 7.5, 300 mM NaCl, 40 mM imidazole, 10 mM 2-mercaptoethanol, and 20% glycerol. BciD was eluted with a minimal volume of elution buffer, which was the same as the wash buffer except for the imidazole concentration (250 mM). The dark brown-colored fractions were pooled and concentrated using an Amicon stirred ultrafiltration cell with a YM-10 filter (10,000 molecular weight cut-off; Millipore, Bedford, MA). The protein was exchanged into storage buffer containing 50 mM HEPES, pH 7.5, 100 mM NaCl, 10 mM dithiothreitol, and 20% glycerol using PD-10 gel filtration columns (GE Healthcare) and stored in aliquots in liquid nitrogen.

Protein Analyses and Verification—The purity of the BciD-His$_6$ protein was assessed by electrophoresis on 12% (w/v) polyacrylamide gels in the presence of SDS; proteins were stained with Coomassie Blue R-250 (65). The identity of purified BciD-His$_6$ was verified by in-gel trypsin digestion (66) accompanied by mass spectrometry at the Proteomics and Mass Spectrometry Core Facility (The Pennsylvania State University, University Park, PA). Protein concentrations were determined by the Bradford assay using a BSA standard (67). Quantitative amino acid analysis performed by the University of California-Davis Proteomics Core Facility established that a correction factor of 0.87 was necessary for protein concentrations determined by the Bradford assay.

Reconstitution of Fe/S Cluster—The reconstitution procedure (48, 68, 69) was carried out on ice with gentle stirring in an anoxic chamber. A final concentration of dithiothreitol (2 mg ml^{-1}) was added to reconstitution buffer (100 mM HEPES, pH 7.5, 300 mM NaCl, 10% (v/v) glycerol), and the solution was incubated for 10 min before adding 300 μM FeCl$_3$. Purified BciD-His$_6$ was added to a final concentration of 30 μM, and the solution was incubated for 1 h. A Na$_2$S solution (100 mM) was slowly added to the protein solution over a 3-h period to produce a final concentration of 300 μM, and the resulting reaction

mixture was incubated on ice for 12 h. The protein solution was centrifuged at $10,000 \times g$ for 10 min, and the supernatant was concentrated and exchanged into storage buffer. To remove adventitiously bound iron, BciD-His$_6$ was chromatographed on a Superdex 75 10/300 GL size exclusion column (GE Healthcare) maintained in an anoxic chamber.

Spectroscopic Measurements—UV-visible absorbance spectra of protein and pigment samples were measured on a GENESYS 10 spectrophotometer (ThermoFisher Scientific Corp., Waltham, MA). Spectra of protein samples were measured in quartz cuvettes that were sealed inside an anoxic chamber.

For EPR measurements, samples of as-isolated and reconstituted BciD-His$_6$ were transferred to EPR tubes in storage buffer. To characterize the presence of Fe/S cluster(s), each protein preparation was measured in both the untreated and reduced states. To reduce the Fe/S cluster(s) fully, dithionite in storage buffer was added to a final concentration of 5 mM to the appropriate protein samples, and the samples were then frozen in liquid nitrogen. EPR spectra were collected using a cylindrical TE 011 mode resonator and a Bruker E500 spectrometer (Bruker Biospin Corp., Billerica, MA) at X-band (9.39 GHz). The temperature was maintained using an ESR 900 liquid helium cryostat and an ITC-4 temperature controller (Oxford Instruments, Concord, MA). EPR spectra were recorded at 15 K at 0.2-milliwatt microwave power with modulation amplitude of 20 G (2 millitesla) at a modulation frequency of 100 kHz. Sixteen scans were collected and averaged for each sample; the difference spectrum was calculated by subtracting the spectrum for the untreated protein from that for the dithionite-reduced protein.

Pigment Separation and Preparation of Substrate Compounds—Pigments were separated and analyzed by reversed-phase HPLC using a 25 cm × 4.6-mm Discovery 5-μm C-18 column (Supelco, Bellefonte, PA) and an Agilent series 1100 HPLC system equipped with a diode array detector (Agilent Technologies, Palo Alto, CA) (70). The data were analyzed using Agilent ChemStation software (revision B.02.01-SR1 6100 series). Pigment samples or reaction products were filtered through a 0.2-μm syringe filter, and 10 mM ammonium acetate was added before injection onto the column. Previously described separation methods (71–73) were modified slightly to separate the BChlide and bacteriopheophorbide (BPheide) components of interest. The column was pre-equilibrated with 12% solvent B (methanol, ethyl acetate, acetonitrile, 50:30:20 (v/v/v)) and 88% solvent A (methanol, 1 M ammonium acetate, 70:30 (v/v)) at a flow rate of 0.75 ml min^{-1} at injection and maintained for 5 min. After 5 min, solvent B was increased linearly to 43%, and the flow rate was increased linearly to 1 ml min^{-1} at 44 min. Solvent B was linearly increased to 100% from 44 to 55 min and then held constant for 10 min. The column was then returned to 12% solvent B and washed extensively before the next injection.

BChlide *c* was prepared from a 2-liter culture of the *bciD* mutant of *C. limnaeum* (see "Results"), and BChlide *d* was prepared from a 2-liter culture of the *bchU* mutant of *C. tepidum* (12). Cells were harvested by centrifugation, and pigments were extracted with 7:2 acetone/methanol (40 ml) for 1 h at room temperature in the dark with stirring. Cell debris was removed

by centrifugation, and the solubilized pigments were purified using a previously described, reversed-phase HPLC method (13). The BChl fractions were collected, pooled, dried under liquid nitrogen, washed with acetone, and finally dried again. To hydrolyze the esterifying alcohol groups of the BChls, the dried pigments were suspended in 4:1 solution of acetone/water containing 0.1 M NaOH, and the solution was incubated in the dark for 3 h (53). One volume of hexane was added to extract unreacted BChls, and the acetone layer was dried under liquid nitrogen and washed three times with acetone. Dried samples were stored at $-20\,°C$ until required.

Mass Spectrometry—Mass spectrometric analysis was performed on a Waters Q-TOF Premier quadrupole/time-of-flight mass spectrometer (Waters Corp. (Micromass Ltd.), Manchester, UK). MassLynx^{TM} software version 4.1 was used to operate the mass spectrometer. Samples were introduced into the mass spectrometer using a Waters 2695 high performance liquid chromatograph. The separation was performed using the same HPLC column and solvent gradient described above for analysis of the reaction products. The samples were resuspended in acetonitrile (100 μl) and vortexed until dissolved. The injection volume was 25 μl. The nitrogen drying gas temperature was set to 300 °C at a flow of 7 liters min^{-1}, and the capillary voltage was 2.8 kV. The mass spectrometer was set to scan from 400 to 700 m/z in positive ion mode, using electrospray ionization. Data acquisition was performed in the middle of the run, dependent upon the anticipated elution time of the analytes.

Enzyme Activity Assay—Enzyme assays were performed inside an anoxic chamber in the dark at room temperature. The reaction buffer consisted of 100 mM MOPS, pH 8.0, 100 mM NaCl. Tryptophan (200 μM final concentration) was added as an internal standard. In addition, a final concentration of 700 μM SAM and 1 mM dithionite were added as cofactor and reductant, respectively. Reactions contained a final concentration of 0.2 mg ml^{-1} purified BciD; an equal volume of enzyme storage buffer was added to control reactions. BChlide *c* (final concentration, 0.05 mg ml^{-1}) or BChlide *d* (final concentration, 0.18 mg ml^{-1}) in acetone was added to the enzyme solution to start the reaction. At appropriate times, aliquots were removed from each reaction for analysis. An equal volume of cold acetone was added to stop the reaction, and precipitated protein was pelleted by centrifugation. Samples were stored on ice or at $-20\,°C$ until the pigments were analyzed by reversed-phase HPLC.

To analyze SAM-related products, separate aliquots were taken at each time point, and an equal volume of 100 mM H$_2$SO$_4$ was added to stop the reaction. SAM products were separated by a reversed-phase HPLC procedure modified from Lanz *et al.* (48), using a 150 × 4.6-mm Kinetex 5-μm C-18 column (Phenomenex Inc., Torrance, CA) and a Shimadzu UFLC system (Shimadzu Scientific Instruments, Columbia, MD). Reaction products were filtered through a syringe filter (0.2 μm) before being injected onto the column. The column was pre-equilibrated with 2% solvent B (HPLC grade acetonitrile) and 98% solvent A (5% methanol, 40 mM ammonium acetate, pH 6.2) at a flow rate of 0.5 ml min^{-1} at injection and maintained for 6.5 min. Solvent B was increased linearly to 12% from 6.5 to 25 min,

then to 24% from 25 to 33 min, and finally to 50% from 33 to 40 min. Solvent B was maintained at 50% for 10 min and then returned to the starting conditions. Products were monitored by UV-visible detection at 260 nm and were compared with authentic standards for SAM and 5′-deoxyadenosine.

Phylogenetic Analyses—Phylogenetic relationships were inferred by the maximum likelihood method based on the JTT matrix-based model (74). The tree with the highest log likelihood value ($-10{,}582.4753$) is shown. Based upon 100 bootstrap resamplings of the data, the percentage of trees in which the associated taxa clustered together is indicated next to the branches. Initial tree(s) for the heuristic search were obtained automatically by applying neighbor-joining and BioNJ algorithms to a matrix of pairwise distances that were estimated using a JTT model and then by selecting the topology with the highest log likelihood value. The tree is drawn to scale, with branch lengths scaled to the number of substitutions per site. The analysis employed 52 amino acid sequences. All positions containing gaps due to insertions/deletions were eliminated from the alignment. The final alignment data set contained 244 positions. Evolutionary analyses were conducted in MEGA7 (75).

Author Contributions—J. L. T. designed and performed the experiments, interpreted the data, and wrote the initial draft of the manuscript; B. H. F. performed the electron paramagnetic resonance measurements; and J. H. G. assisted in the interpretation of the EPR data and edited the manuscript. D. A. B. conceived the project, directed the research, assisted in the interpretation of the data, and wrote and edited the manuscript. All authors approved the final version of the manuscript.

References

1. Bryant, D. A., and Frigaard, N.-U. (2006) Prokaryotic photosynthesis and phototrophy illuminated. *Trends Microbiol.* **14,** 488–496

2. Bryant, D. A., Costas, A. M., Maresca, J. A., Chew, A. G., Klatt, C. G., Bateson, M. M., Tallon L. J., Hostetler, J., Nelson, W. C., Heidelberg, J. F., and Ward, D. M. (2007) "*Candidatus* Chloracidobacterium thermophilum": an aerobic phototrophic acidobacterium. *Science* **317,** 523–526

3. Bryant, D. A., Liu, Z., Li, T., Zhao, F., Garcia Costas, A. M., Klatt, C. G., Ward, D. M., Frigaard, N.-U., and Overmann, J. (2012) Comparative and functional genomics of anoxygenic green bacteria from the taxa *Chlorobi, Chloroflexi,* and *Acidobacteria.* In *Advances in Photosynthesis and Respiration,* Vol. 35 (Burnap, R. L., and Vermaas, W., eds) pp. 47–102, Springer, Dordrecht, Netherlands

4. Frigaard, N.-U., and Bryant, D. A. (2006) Chlorosomes: antenna organelles in green photosynthetic bacteria. In: *Complex Intracellular Structures in Prokaryotes* (Shively, J. M., ed) pp. 79–114, Springer, Berlin

5. Oostergetel, G. T., van Amerongen, H., and Boekema, E. J. (2010) The chlorosome: a prototype for efficient light harvesting in photosynthesis. *Photosynth. Res.* **104,** 245–255

6. Orf, G. S., and Blankenship, R. E. (2013) Chlorosome antenna complexes from green photosynthetic bacteria. *Photosynth. Res.* **116,** 315–331

7. Montaño, G. A., Bowen, B. P., LaBelle, J. T., Woodbury, N. W., Pizziconi, V. B., and Blankenship, R. E. (2003) Characterization of *Chlorobium tepidum* chlorosomes: a calculation of bacteriochlorophyll *c* per chlorosome and oligomer modeling. *Biophys. J.* **85,** 2560–2565

8. Bryant, D. A., Vassilieva, E. V., Frigaard, N.-U., and Li, H. (2002) Selective protein extraction from *Chlorobium tepidum* chlorosomes using detergents: evidence that CsmA forms multimers and binds bacteriochlorophyll *a. Biochemistry* **41,** 14403–14411

9. Adams, P. G., Cadby, A. J., Robinson, B., Tsukatani, Y., Tank, M., Wen, J., Blankenship, R. E., Bryant, D. A., and Hunter, C. N. (2013) Comparison of the physical characteristics of chlorosomes from three different phyla of green phototrophic bacteria. *Biochim. Biophys. Acta* **1827,** 1235–1244

10. Manske, A. K., Glaeser, J., Kuypers, M. M., and Overmann, J. (2005) Physiology and phylogeny of green sulfur bacteria forming a monospecific phototrophic assemblage at a depth of 100 meters in the Black Sea. *Appl. Environ. Microbiol.* **71,** 8049–8060

11. Marschall, E., Jogler, M., Hessge, U., and Overmann, J. (2010) Large-scale distribution and activity patterns of an extremely low-light-adapted population of green sulfur bacteria in the Black Sea. *Environ. Microbiol.* **12,** 1348–1362

12. Maresca, J. A., Gomez Maqueo Chew, A., Ponsatí, M. R., Frigaard, N.-U., Ormerod, J. G., Jones, A. D., and Bryant, D. A. (2004) The *bchU* gene of *Chlorobium tepidum* encodes the bacteriochlorophyll C-20 methyltransferase. *J. Bacteriol.* **186,** 2558–2566

13. Vogl, K., Tank, M., Orf, G. S., Blankenship, R. E., and Bryant, D. A. (2012) Bacteriochlorophyll *f*: properties of chlorosomes containing the "forbidden chlorophyll." *Front. Microbiol.* **3,** 298

14. Orf, G. S., Tank, M., Vogl, K., Niedzwiedzki, D. M., Bryant, D. A., and Blankenship, R. E. (2013) Spectroscopic insights into the decreased efficiency of chlorosomes containing bacteriochlorophyll *f. Biochim. Biophys. Acta* **1827,** 493–501

15. Niedzwiedzki, D. M., Orf, G. S., Tank, M., Vogl, K., Bryant, D. A., and Blankenship, R. E. (2014) Photophysical properties of the excited states of bacteriochlorophyll *f* in solvents and in chlorosomes. *J. Phys. Chem. B* **118,** 2295–2305

16. Harada, J., Mizoguchi, T., Tsukatani, Y., Noguchi, M., and Tamiaki, H. (2012) A seventh bacterial chlorophyll driving a large light-harvesting antenna. *Sci. Rep.* **2,** 671

17. Tsukatani, Y., Harada, J., Mizoguchi, T., and Tamiaki, H. (2013) Bacteriochlorophyll homolog compositions in the *bchU* mutants of green sulfur bacteria. *Photochem. Photobiol. Sci.* **12,** 2195–2201

18. Chew, A. G., and Bryant, D. A. (2007) Chlorophyll biosynthesis in bacteria: the origins of structural and functional diversity. *Annu. Rev. Microbiol.* **61,** 113–129

19. Eisen, J. A., Nelson, K. E., Paulsen, I. T., Heidelberg, J. F., Wu, M., Dodson, R. J., Deboy, R., Gwinn, M. L., Nelson, W. C., Haft, D. H., Hickey, E. K., Peterson, J. D., Durkin, A. S., Kolonay, J. L., Yang, F., *et al.* (2002) The complete genome sequence of the green sulfur bacterium *Chlorobium tepidum. Proc. Natl. Acad. Sci. U.S.A.* **99,** 9509–9514

20. Frigaard, N.-U., Voigt, G. D., and Bryant, D. A. (2002) A bacteriochlorophyll *c*-less mutant of *Chlorobium tepidum* made by inactivation of the *bchK* gene encoding bacteriochlorophyll *c* synthase. *J. Bacteriol.* **184,** 3368–3376

21. Gomez Maqueo Chew, A., Frigaard, N.-U., and Bryant, D. A. (2005) Characterization of BchV, a C-3^1 hydratase specific for hypermethylated bacteriochlorophyll *c* in *Chlorobium tepidum.* In *Photosynthesis: Fundamental Aspects to Global Perspectives* (van der Est, A., and Bruce, D., eds) pp. 875–877, Allen Press, Lawrence, KS

22. Gomez Maqueo Chew, A., Frigaard, N.-U., and Bryant, D. A. (2007) Bacteriochlorophyllide *c* C-8^2 and C-12^1 methyltransferases are essential for adaptation to low light in *Chlorobaculum tepidum. J. Bacteriol.* **189,** 6176–6184

23. Liu, Z., and Bryant, D. A. (2011) Identification of a gene essential for the first committed step in the synthesis of bacteriochlorophyll *c. J. Biol. Chem.* **286,** 22393–22402

24. Liu, Z., and Bryant, D. A. (2012) Biosynthesis and assembly of bacterio-chlorophyll *c* in green bacteria: theme and variations. In *Handbook of Porphyrin Science*, Vol. 20, (Kadish, K. M., Smith, K. M., Guilard, R., eds) pp. 108–142, World Scientific Publishing, Hackensack, NJ

25. Bryant, D. A., and Liu, Z. (2013) Green bacteria: insights into green bacterial evolution through genomic analyses in *Advances in Botanical Research. In Genome Evolution of Photosynthetic Bacteria* (Beatty, J. T., ed.), Vol. 66, pp. 99–150, Elsevier, New York, NY

26. Teramura, M., Harada, J., Mizoguchi, T., Yamamoto, K., and Tamiaki, H. (2016) *In vitro* assays of BciC showing C13^2-demethoxycarbonylase activity requisite for biosynthesis of chlorosomal chlorophyll pigments. *Plant Cell Physiol.* **57,** 1048–1057

27. Gomez Maqueo Chew, A., Frigaard, N.-U., and Bryant, D. A. (2005) Characterization of BchV, a C-3^1 hydratase specific for hypermethylated bacteriochlorophyll *c* in *Chlorobium tepidum.* In *Photosynthesis: Fundamental Aspects to Global Perspectives* (van der Est, A., and Bruce, D., eds) pp. 875–877, Allen Press, Lawrence, KS

28. Harada, J., Teramura, M., Mizoguchi, T., Tsukatani, Y., Yamamoto, K., and Tamiaki, H. (2015) Stereochemical conversion of C3-vinyl group to 1-hydroethyl group in bacteriochlorophyll *c* by the hydratases BchF and BchV: adaptation of green sulfur bacteria to light-limited environments. *Mol. Microbiol.* **98,** 1184–1198

29. Teramura, M., Harada, J., and Tamiaki, H. (2016) *In vitro* stereospecific hydration activities of the 3-vinyl group of chlorophyll derivatives by BchF and BchV enzymes involved in bacteriochlorophyll *c* biosynthesis of green sulfur bacteria. *Photosynth. Res.* **130,** 33–45

30. Harada, J., Saga, Y., Yaeda, Y., Oh-Oka, H., and Tamiaki, H. (2005) *In vitro* activity of C-20 methyltransferase, BchU, involved in bacteriochlorophyll *c* biosynthetic pathway in green sulfur bacteria. *FEBS Lett.* **579,** 1983–1987

31. Wada, K., Yamaguchi, H., Harada, J., Niimi, K., Osumi, S., Saga, Y., Oh-Oka, H., Tamiaki, H., and Fukuyama, K. (2006) Crystal structures of BchU, a methyltransferase involved in bacteriochlorophyll *c* biosynthesis, and its complex with *S*-adenosylhomocysteine: implications for reaction mechanism. *J. Mol. Biol.* **360,** 839–849

32. Broch-Due, M., and Ormerod, J. G. (1978) Isolation of a BCHL *c* mutant from *Chlorobium* with BCHL *d* by cultivation at low light intensity. *FEMS Microbiol. Lett.* **3,** 305–308

33. Bobe, F. W., Pfennig, N., Swanson, K. L., and Smith, K. M. (1990) Red shift of absorption maxima in *Chlorobineae* through enzymic methylation of their antenna bacteriochlorophylls. *Biochemistry* **29,** 4340–4348

34. Saga, Y., and Tamiaki, H. (2004) Comparison between chlorosomes containing bacteriochlorophyll-*c* and and chlorosomes containing bacteriochlorophyll-*d* isolated from two substrains of green sulfur photosynthetic bacterium *Chlorobium vibrioforme* NCIB 8327. *J. Photochem. Photobiol. B* **75,** 89–97

35. Harada, J., Oh-Oka, H., Saga, Y., and Tamiaki, H. (2005) Natural reverse mutations of the inactivated *bchU* gene in *Chlorobium vibrioforme* NCIB 8327. In *Photosynthesis: Fundamental Aspects to Global Perspectives* (van der Est, A., Bruce, D., eds) pp. 119–120, Allen Press, Lawrence, KS

36. Scheer, H. (2006) An overview of chlorophylls and bacteriochlorophylls: biochemistry, biophysics, functions and applications. In *Advances in Photosynthesis and Respiration*, Vol. 25 (Grimm, B., Porra, R. J., Rüdiger, W., and Scheer, H., eds) pp. 1–26, Springer, Dordrecht, Netherlands

37. Tanaka, A., Ito, H., Tanaka, R., Tanaka, N. K., Yoshida, K., and Okada, K. (1998) Chlorophyll *a* oxygenase (CAO) is involved in chlorophyll *b* formation from chlorophyll *a*. *Proc. Natl. Acad. Sci. U.S.A.* **95,** 12719–12723

38. Tomitani, A., Okada, K., Miyashita, H., Matthijs, H. C., Ohno, T., and Tanaka, A. (1999) Chlorophyll *b* and phycobilins in the common ancestor of cyanobacteria and chloroplasts. *Nature* **400,** 159–162

39. Maresca, J. A. (2007) The genetic basis for pigment variation among green sulfur bacteria. Ph.D. thesis, The Pennsylvania State University

40. Llorens-Marès, T., Liu, Z., Allen, L. Z., Rusch, D. B., Craig, M. T., Dupont, C. L., Bryant, D. A., and Casamayor, E. O. (2017) Speciation and ecological success in dimly lit waters: horizontal gene transfer in a green sulfur bacteria bloom unveiled by metagenomic assembly. *ISME J.* **11,** 201–211

41. Yang, J., Kulkarni, K., Manolaridis, I., Zhang, Z., Dodd, R. B., Mas-Droux, C., and Barford, D. (2011) Mechanism of isoprenylcysteine carboxylmethylation from the crystal structure of the integral membrane methyltransferase ICMT. *Mol. Cell* **44,** 997–1004

42. Maresca, J. A., Romberger, S. P., and Bryant, D. A. (2008) Isorenieratene biosynthesis in green sulfur bacteria requires the cooperative actions of two carotenoid cyclases. *J. Bacteriol.* **190,** 6384–6391

43. Wang, J., Woldring, R. P., Román-Meléndez, G. D., McClain, A. M., Alzua, B. R., and Marsh, E. N. (2014) Recent advances in radical SAM enzymology: new structures and mechanisms. *ACS Chem. Biol.* **9,** 1929–1938

44. Ouchane, S., Steunou, A.-S., Picaud, M., and Astier, C. (2004) Aerobic and anaerobic Mg-protoporphyrin monomethyl ester cyclases in purple bacteria. *J. Biol. Chem.* **279,** 6385–6394

45. Chen, G. E., Canniffe, D. P., Martin, E. C., and Hunter, C. N. (2016) Absence of the *cbb*$_3$ terminal oxidase reveals an active oxygen-dependent cyclase involved in bacteriochlorophyll biosynthesis in *Rhodobacter sphaeroides*. *J. Bacteriol.* **198,** 2056–2063

46. Harada, J., Mizoguchi, T., Satoh, S., Tsukatani, Y., Yokono, M., Noguchi, M., Tanaka, A., and Tamiaki, H. (2013) Specific gene *bciD* for C7-methyl oxidation in bacteriochlorophyll *e* biosynthesis of brown-colored green sulfur bacteria. *PLoS One* **8,** e60026

47. Imhoff, J. F. (2003) Phylogenetic taxonomy of the family *Chlorobiaceae* on the basis of 16S rRNA and *fmo* (Fenna-Matthews-Olson protein) gene sequences. *Int. J. Syst. Evol. Microbiol.* **53,** 941–951

48. Lanz, N. D., Grove, T. L., Gogonea, C. B., Lee, K. H., Krebs, C., and Booker, S. J. (2012) RlmN and AtsB as models for the overproduction and characterization of radical SAM proteins. *Methods Enzymol.* **516,** 125–152

49. Yoon, K.-S., Bobst, C., Hemann, C. F., Hille, R., and Tabita, F. R. (2001) Spectroscopic and functional properties of novel 2[4Fe4S] cluster-containing ferredoxins from the green sulfur bacterium *Chlorobium tepidum*. *J. Biol. Chem.* **276,** 44027–44036

50. Seo, D., Tomioka, A., Kusumoto, N., Kamo, M., Enami, I., and Sakurai, H. (2001) Purification of ferredoxins with purified reaction center complex from the green sulfur bacterium *Chlorobium tepidum*. *Biochim. Biophys. Acta* **1503,** 377–384

51. Oster, U., Bauer, C. E., and Rüdiger, W. (1997) Characterization of chlorophyll *a* and bacteriochlorophyll *a* synthetases by heterologous expression in *E. coli. J. Biol. Chem.* **272,** 9671–9676

52. Suzuki, J. Y., Bollivar, D. W., and Bauer, C. E. (1997) Genetic analysis of chlorophyll biosynthesis. *Annu. Rev. Genet.* **31,** 61–89

53. Saga, Y., Hirota, K., Harada, J., and Tamiaki, H. (2015) *In vitro* enzymatic activities of bacteriochlorophyll *a* synthase derived from the green sulfur photosynthetic bacterium *Chlorobaculum tepidum*. *Biochemistry* **54,** 4998–5005

54. Montesinos, E., Guerrero, R., Abella, C., and Esteve, I. (1983) Ecology and physiology of the competition for light between *Chlorobium limicola* and *Chlorobium phaeobacteroides*. *Appl. Environ. Microbiol.* **46,** 1007–1016

55. Vila, X., and Abella, C. A. (2001) Light-harvesting adaptations of planktonic phototrophic microorganisms to different light quality conditions. *Hydrologia* **452,** 15–30

56. van Gemerden, H., and Mas, J. (1995) Ecology of phototrophic sulfur bacteria. In *Advances in Photosynthesis and Respiration*, Vol. 2 (Blankenship, R. E., Madigan, M. T., and Bauer, C. E., eds) pp. 49–85, Springer, Dordrecht, Netherlands

57. Liu, Z., Klatt, C. G., Ludwig, M., Rusch, D. B., Jensen, S. I., Kühl, M., Ward, D. M., and Bryant, D. A. (2012) "*Candidatus* Thermochlorobacter aerophilum": an aerobic chlorophotoheterotrophic member of the phylum *Chlorobi*. *ISME J.* **6,** 1869–1882

58. Tank, M., Thiel, V. Ward, D. M., and Bryant, D. A. (2016) A panoply of phototrophs: a photomicrographic overview of chlorophototrophs found in the microbial mats of alkaline siliceous hot springs in Yellowstone National Park, WY, U.S.A. In *Modern Topics in the Phototrophic Prokaryotes: Environmental and Applied Aspects* (Hallenbeck, P. C., ed) Springer, Berlin, in press.

59. Akiva, E., Brown, S., Almonacid, D. E., Barber, A. E., 2nd, Custer, A. F., Hicks, M. A., Huang, C. C., Lauck, F., Mashiyama, S. T., Meng, E. C., Mischel, D., Morris, J. H., Ojha, S., Schnoes, A. M., Stryke, D., *et al.* (2014) The structure-function linkage database. *Nucleic Acids Res.* **42,** D521–D530

60. Wahlund, T. M., and Madigan, M. T. (1995) Genetic transfer by conjugation in the thermophilic green sulfur bacterium. *Chlorobium tepidum*. *J. Bacteriol.* **177,** 2583–2588

61. Frigaard, N.-U., and Bryant, D. A. (2001) Chromosomal gene inactivation in the green sulfur bacterium *Chlorobium tepidum* by natural transformation. *Appl. Environ. Microbiol.* **67,** 2538–2544

62. Simon, R., Priefer, U., and Pühler, A. (1983) A broad host range mobilization system for *in vivo* genetic engineering: transposon mutagenesis in Gram-negative bacteria. *Nat. Biotechnol.* **1,** 784–791

63. Zheng, L., Cash, V. L., Flint, D. H., and Dean, D. R. (1998) Assembly of iron-sulfur clusters: identification of an *iscSUA-hscBA-fdx* gene cluster from *Azotobacter vinelandii*. *J. Biol. Chem.* **273,** 13264–13272

64. Delli-Bovi, T. A., Spalding, M. D., and Prigge, S. T. (2010) Overexpression of biotin synthase and biotin ligase is required for efficient generation of sulfur-35 labeled biotin in *E. coli. BMC Biotechnol.* **10,** 73

65. Shen, G., and Bryant, D. A. (1995) Characterization of a *Synechococcus* sp. strain PCC 7002 mutant lacking Photosystem I: protein assembly and energy distribution in the absence of the photosystem I reaction center core complex. *Photosynth. Res.* **44,** 41–53

66. Ho, M.-Y., Gan, F., Shen, G., and Bryant, D. A. (2016) Far-red light photoacclimation (FaRLiP) in *Synechococcus* sp. PCC 7335. II. Characterization of phycobiliproteins produced during acclimation to far-red light. *Photosynth. Res.* 10.1007/s11120-016-0303-5

67. Bradford, M. (1976) A rapid and sensitive method for the quantitation of microgram quantities of protein utilizing the principle of protein-dye binding. *Anal. Biochem.* **72,** 248–254

68. Zhao, J. D., Warren, P. V., Li, N., Bryant, D. A., and Golbeck, J. H. (1990) Reconstitution of electron transport in Photosystem I with PsaC and PsaD proteins expressed in *Escherichia coli. FEBS Lett.* **276,** 175–180

69. Lovenberg, W., Buchanan, B. B., and Rabinowitz, J. C. (1963) Studies on the chemical nature of clostridial ferredoxin. *J. Biol. Chem.* **238,** 3899–3913

70. Frigaard, N.-U., Takaichi, M., Hirota, K., Shimada, K., and Matsuura, K. (1997) Quinones in chlorosomes of green sulfur bacteria and their role in the redox-dependent fluorescence studied in chlorosome-like bacteriochlorophyll *c* aggregates. *Arch. Microbiol.* **167,** 343–349

71. Borrego, C. M., and Garcia-Gil, L. J. (1994) Separation of bacteriochlorophyll homologues from green photosynthetic bacteria by reversed-phase HPLC. *Photosynth. Res.* **41,** 157–164

72. Borrego, C. M., Gerola, P. D., Miller, M., and Cox, R. P. (1999) Light intensity effects on pigment composition and organization in the green sulfur bacterium *Chlorobium tepidum. Photosynth. Res.* **59,** 159–166

73. Mallorquí, N., Arellano, J. B., Borrego, C. M., and Garcia-Gil, L. J. (2005) Signature pigments of green sulfur bacteria in lower Pleistocene deposits from the Banyoles lacustrine area (Spain). *J. Paleolimnol.* **34,** 271–280

74. Jones, D. T., Taylor, W. R., and Thornton, J. M. (1992) The rapid generation of mutation data matrices from protein sequences. *Comput. Appl. Biosci.* **8,** 275–282

75. Kumar, S., Stecher, G., and Tamura, K. (2016) MEGA7: Molecular Evolutionary Genetics Analysis version 7.0 for bigger datasets. *Mol. Biol. Evol.* **33,** 1870–1874